

Temporal Cooperativity and Sensitivity Amplification in Biological Signal Transduction[†]

Hong Qian^{*,‡} and Jonathan A. Cooper^{*,§}

Department of Applied Mathematics, University of Washington, Seattle, Washington 98195, and Division of Basic Sciences, Fred Hutchinson Cancer Research Center, Seattle, Washington 98109

Received October 23, 2007; Revised Manuscript Received December 10, 2007

ABSTRACT: Sensitivity amplification in signal transduction modules regulated by phosphorylation–dephosphorylation cycles and GTPases results from a new type of cooperativity which is fundamentally different from that of allosterism. This type of cooperativity, termed temporal cooperativity [Qian, H. (2003) *Biophys. Chem.* 105, 585–593], is analyzed in this paper through stochastic models for molecular interactions. Mathematical analysis is developed through a series of models with different levels of complexity, from which a simple conceptual model based on linear cooperativity is derived. The following are shown: (i) When both kinase and phosphatase are nonsaturating, the distribution of the number of activated substrate molecules is binomial. With increasing kinase activity, the peak of the distribution continuously moves toward 100% activation. (ii) When the kinase is saturated, i.e., zeroth order, the distribution is Poisson. (iii) When both enzymes are saturated, the distribution is geometric. Ultrasensitivity corresponds to an abrupt switching of the peak position of the distribution from 0 to 100%. The theory is applicable to a wide range of processes in cell signaling including the specificity and sensitivity of T-cell activation.

Protein phosphorylation is one of the most important biochemical reactions in living cells (1, 2). The biological activity of a protein is often “turned on” by the phosphorylation, catalyzed by a specific kinase, and “turned off” by a dephosphorylation reaction, catalyzed usually by a specific phosphatase. The sequential events of turning on and off enzyme activities constitute the primary mechanism of information propagation in biochemical terms inside a cell, from the precisely programmed “instructions” in a genome to cellular functions. This is known as biochemical signal transduction.

The turning on and off of the biological activity of a protein has been widely recognized as a switch in controlling information flow. This mechanism is now one of the key concepts in cellular biology. The basic chemical reactions of this all-important, simple biochemical “network”, thus, can and should be completely studied in quantitative terms. The first mathematical model of the phosphorylation–dephosphorylation cycle (PdPC¹) was developed by Stadtman and Chock (3). Goldbeter and Koshland (4) have discovered the ultrasensitivity of a PdPC switch in terms of the zeroth-

order kinetics of kinase and phosphatase. Qian has further elucidated the importance of open-system chemical reaction, in terms of continuous ATP hydrolysis, in the proper functioning of such a switch (5, 6). Gonze and Goldbeter (7) and Heinrich et al. (8) have studied mathematical models for kinase signal transduction networks. The switch characteristics, the ultrasensitive activation, and the open-system nature of the PdPC module all have been experimentally demonstrated in test tube with ATP regenerating system (9–11). A wide range of experiments in cells have further established the importance of this reaction system. See a recent paper and the references within (12).

One of the key concepts in the PdPC signaling is the switching sensitivity: the sharpness of the activation of the substrate protein in response to the increasing activity of the kinase (or phosphatase, depending on the actual biological setting). One of the observations is that in the case of the kinase being highly saturated by the substrate protein, i.e., the kinase-catalyzed reaction is zeroth order, the switch exhibits high sensitivity (4).

The biochemical network of PdPC is also closely related to several other important biochemical systems currently under intense investigation. These include membrane bound GTPase system (13, 14) and the activation of the T-cell receptors (TCR) by the antigen-major histocompatibility complex (MHC) on antigen-presenting cells (APC) (15). Figure 1 shows PdPC and GTPase systems with isomorphic kinetics. Tan et al. in fact have examined the ultrasensitivity in a GTPase system, that of Rac1 with GEF Trio and GAP p50Rho (16).

Sensitivity is usually understood as a sharp response to a small change in the signal strength in terms of kinase/

[†] Supported in part by NIH Grants GM068610 for H.Q. and R01-CA41072 to J.A.C.

^{*} Authors to whom correspondence should be addressed. H.Q.: (206) 543-2584 (tel), (206) 616-1440 (fax), qian@amath.washington.edu. J.A.C.: (206) 667-4454 (tel), (206) 667-6522 (fax), jcooper@fhcrc.org.

[‡] University of Washington.

[§] Fred Hutchinson Cancer Research Center.

¹ Abbreviations: ADP, adenosine diphosphate; ATP, adenosine triphosphate; APC, antigen-presenting cell; GAP, GTPase-activating protein; GDP, guanosine diphosphate; GEF, guanine nucleotide exchange factor; GTP, guanosine triphosphate; MHC, major histocompatibility complex; MMBH, Michaelis–Menten–Briggs–Haldane; PdPC, phosphorylation–dephosphorylation cycle; TCR, T-cell receptor.

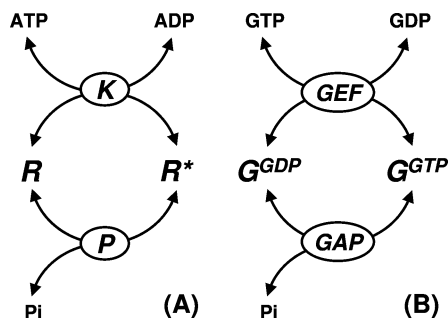


FIGURE 1: Even though biochemically PdPC in (A) and GTPase in (B) are widely considered to be different, each with its own significant roles to play in cellular signaling, their kinetics is isomorphic as shown here. In (A) R and R* are the unphosphorylated and phosphorylated forms of a protein; K and P stand for kinase and phosphatase. In (B) G^{GDP} and G^{GTP} are GTPase with bound GDP and GTP, respectively; GEF and GAP stand for guanine nucleotide exchange factor and GTPase-activating protein.

phosphatase concentrations or activities. If the kinase/phosphatase activities are regulated by a ligand binding to a receptor, then the PdPC sensitivity becomes intimately related to the specificity of the ligand induced activation. Both sensitivity and specificity are key issues in the studies of T-cell activation (15, 17). There, one has observed high sensitivity due to very few copies of the antigen-MHC complex on the APC, and high specificity in T-cell response to different antigens. Various models, i.e., serial engagement and kinetic proofreading, have been considered. As we shall show, all these different biological signaling processes can be better understood in terms of a stochastic kinetic model for the PdPC and its variations.

A thorough understanding of the PdPC-like network kinetics, therefore, is relevant not only to the kinase signaling but also to other cellular signaling networks. In this paper, a series of models with different level of complexity are presented and their quantitative relations investigated. For a highly saturated kinase, there is no competition between kinase molecules for their substrates. Hence the phosphorylation reaction is essentially a single-enzyme process, which can be subjected to mathematical models developed in the field of single molecule enzymology (18). Such a stochastic model for PdPC was introduced in (5), but a detailed analysis has not yet been developed. Our modeling approach is also novel; with a little more complicated algebra it can also be applied to many other signaling systems. We give an example for the activation of T-cell in the later part of the paper; other possible systems are Rabaptin5 dependent membrane Rab5 GTPase activation (19) and G-protein mediated phototransduction in photoreceptors (20).

The present analysis also emphasizes the open-system nature of the biochemical reaction network (6). Having sustained ATP and ADP concentrations with constant phosphorylation potential is essential to the behavior and function of PdPC as a biochemical switch in living cells (5, 21). As we shall show, the thermodynamic energy aspect of the signal transduction plays an important role in further understanding the function of both the PdPC switch and T-cell activation (22).

TWO LEVELS OF KINETIC MODELS FOR PDPC

There are two ways to model PdPC kinetics: one is at the traditional enzyme kinetic level, which is more appropri-

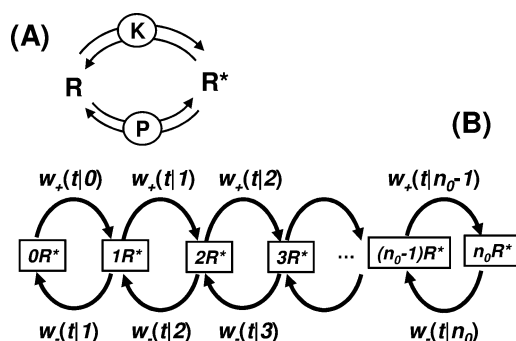


FIGURE 2: (A) Phosphorylation–dephosphorylation cycle (PdPC) in the traditional schematic. Substrate protein R can be phosphorylated to become R*. The phosphorylation and dephosphorylation reactions are catalyzed by two enzymes: kinase K and phosphatase P. Note that the reverse chemical reaction of the phosphorylation is the kinase catalyzed ATP synthesis, *not* dephosphorylation, and the reverse chemical reaction of the dephosphorylation is addition of inorganic phosphate. (B) PdPC in terms of the sequential events of phosphorylation and dephosphorylation of each individual substrate molecule, one at a time. There are totally n_0 substrate protein molecules. In quantitative terms, the *random-walk* model is characterized by the $w_+(t|n)$ and $w_-(t|n)$ ($0 \leq n \leq n_0$): the probability distribution for the dwell times of the system in state nR^* , moving a step forward and backward respectively.

ate for test tube experiments, and one at the stochastic level, which is more appropriate for a small number of kinase molecules, such as in a cell.

Traditional Enzyme Kinetic Model. The first level of kinetic model for the PdPC has been developed by Stadtman and Chock, Goldbeter and Koshland, and Qian (3–5). This is a small biochemical network of three proteins with kinetics shown in Figure 1A and simplified in Figure 2A: The protein R can be phosphorylated to become R*. Both phosphorylation and dephosphorylation are enzyme-catalyzed reactions, with kinase (K) and phosphatase (P) respectively. Enzymatic reactions are modeled according to the reversible Michaelis–Menten–Briggs–Haldane (MMBH) mechanism.

According to (4), “ultrasensitive” and “subsensitive” responses are defined with respect to a hyperbolic response. The latter is what one expects from a PdPC with both kinase and phosphatase operating in the irreversible, nonsaturating first-order regime (6, 22). In comparison, with zeroth-order phosphorylation catalyzed by the kinase and first-order dephosphorylation catalyzed by the phosphatase, the steady-state of the system in Figure 2A is given in eq 8 herein. Figure 3 shows the fraction of phosphorylation, $f = [R^*]/([R] + [R^*])$, as a function of the activity ratio of the kinase to that of phosphatase θ , the Michaelis constant of the kinase K_M , and the phosphorylation energy $\Delta G = RT \ln \gamma$. f increases with increasing θ and ΔG , and with decreasing K_M .

K_M regulates the sharpness of the activation curve, i.e., sensitivity (4). It can be quantified by the Hill coefficient n_h . For this model n_h is maximally 2, when the kinase is highly saturated (Figure 3A).

ΔG regulates the amplitude of full activation. When $\Delta G = 0$, f is in fact *independent* of the activity of the kinase, as expected from an equilibrium between R and R* which cannot be perturbed by an enzyme (Figure 3B).

Detailed analysis of PdPC with both phosphorylation and dephosphorylation reactions being reversible and zeroth-order can be found in (5). For analysis for irreversible enzymatic

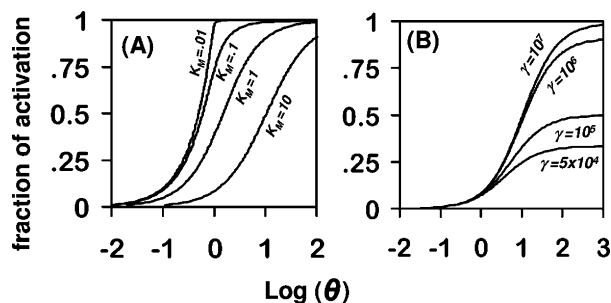


FIGURE 3: The fraction of phosphorylation of a receptor (f) with saturated kinase and nonsaturated phosphatase, as a function of θ , the ratio of the activities of the kinase to that of phosphatase; K_M , the Michaelis constant of the kinase; and $RT \ln \gamma$, the phosphorylation energy from ATP hydrolysis. The curves are plotted according to eq 8. (A) With irreversible kinase and phosphatase ($\mu = \sigma = 0$, $\gamma\mu = \infty$), the activation curve $f(\theta)$ becomes sharper when the kinase is more saturated. For $K_M \rightarrow \infty$, $f = \theta/(K_M + \theta)$ with $n_h = 1$; and for $K_M \rightarrow 0$, $f = (1 + \theta - (1 - \theta)^{1/2})/2$ with $n_h = 2$. (B) With given $K_M = 10$, $\mu = 10^{-5}$ and $\sigma = 0$, the level of full activation $f(\infty)$ increases with the ATP hydrolysis energy $\Delta G = RT \ln \gamma$.

reactions see (4). Again, ΔG regulates the amplitude of the full activation (5, 6, 21), and the Michaelis constants for the kinase and phosphatase regulate the sensitivity of the activation. As we shall show, the sharpness in this case can be much greater than 2. It is in fact proportional to the concentration of the substrate protein.

Stochastic Model in Terms of a 1-Dimensional Random Walk. Qian (5) has suggested that the nature of the zeroth-order ultrasensitivity can be best understood in terms of a more detailed model in terms of the chain of events of phosphorylation and dephosphorylation of each substrate protein, one at a time. This is shown schematically in Figure 2B. In terms of this random-walk model, we follow the stochastic dynamics of the enzyme reaction system by counting the number of substrate molecules being phosphorylated. The state of the system is determined by the numbers of phosphorylated and unphosphorylated substrate molecules.

The dynamics of the model at this level are quantified as follows. At each state, i.e., a square box in Figure 2B, the system will dwell for a certain amount of time before jumping forward or backward. The respective probabilities of jumping forward and backward at time t is $w_+(t|n)$ and $w_-(t|n)$, in which n is the number of R^* molecules in the state. Note that these time distributions are functions of the state: they are dependent upon the numbers of R and R^* . Then we have the total probability

$$\int_0^\infty [w_+(t|n) + w_-(t|n)] dt = 1 \quad (1)$$

Assuming the total of R and R^* molecules is a constant n_0 , then the number of R molecules in state $\{nR^*\}$ will be $n_0 - n$. This mathematical framework for describing the kinetics is known as a semi-Markov process, also known as continuous-time random walk or extended kinetics (23), which has been extensively studied in recent years in connection to motor-protein kinetics and single-molecule enzymology (18, 24–26).

The random-walk representation provides a deeper understanding for the nature of ultrasensitivity (5, 6) in terms of the cooperativity between successive phosphorylation events. The chain of events are noncooperative if and only

if $w_+(t|n)/w_-(t|n) \propto (n_0 - n)/n$ for all n and independent of t (18, 23, 26). This is the case when both kinase and phosphatase are nonsaturating. Hence, each individual substrate protein undergoes PdPC independent of the others.

Whether the enzymes are saturated or not, when there is no energy input, i.e., $\Delta G = RT \ln \gamma = 0$, the random walk is noncooperative (see eq 16). In that case, $w_+(t|n)$ and $w_-(t|n)$ follow the well-known Haldane equation in enzymology (18): Their ratio $w_+(t|n)/w_-(t|n)$ is determined solely by reaction thermodynamics irrespective of detailed kinetics.

We can further see how the system becomes cooperative. Even though the substrate molecules are all monomeric and there is no allosteric cooperativity in the traditional sense, there are interactions between different substrate molecules. When both kinase and phosphatase are abundant, individual substrate molecules fluctuate between R and R^* independently. Hence there is no interaction whatsoever and the PdPC is noncooperative. However, when the kinase is highly saturated, there is a competition of the kinase for phosphorylation between all the substrate molecules in R . Hence, it is clear that if there are more R^* 's, i.e., fewer R 's, the phosphorylation of one R via kinase becomes less competitive. Here is the origin of the cooperativity: more R^* 's make the remaining R 's more likely to become R^* 's. It is also clear that if the kinase reaction is reversible, i.e., the R^* 's can also compete for the kinase with R 's, then the cooperative effect is diminished. Qian has termed this type of interaction “temporal cooperativity” since the sequential states in Figure 2B are adjacent in time rather than in space which is the case in allosteric cooperativity (5, 6). On the other hand, if there is a competitive inhibitor for the kinase, then it effectively reduces the available amount of kinase. Thus it also leads to sensitivity amplification, as has been shown recently (12).

Michaelis–Menten–Briggs–Haldane Kinetics. The probabilities $w_+(t|n)$ and $w_-(t|n)$ can be derived from the standard MMBH kinetics. We leave the mathematical details for the Methods section. In summary, Figure 9 shows how to map the kinetics in Figure 2A to Figure 2B via a detailed kinetic master equation. For the case of one kinase molecule, Figure 9B shows the detailed events between state $\{nR^*\}$ jumping forward to state $\{(n+1)R^*\}$ or jumping backward to state $\{(n-1)R^*\}$. The corresponding probabilities then can be calculated. The calculations provide the following features:

(1) There are two important quantities associated with $w_+(t|n)$: the total probability of jumping forward from state nR^* , $p_+(n)$, irrespective of when the jump occurs, and the mean dwell time for the jump to occur $\langle t_+ \rangle(n)$. Similarly there are $p_-(n)$ and $\langle t_- \rangle(n)$ associated with $w_-(t|n)$:

$$p_\pm(n) = \int_0^\infty w_\pm(t|n) dt, \quad \langle t_\pm \rangle(n) = \frac{1}{p_\pm(n)} \int_0^\infty t w_\pm(t|n) dt \quad (2)$$

(2) If the biochemical reaction network is in an equilibrium buffer, i.e., the amount of ATP, ADP, and P_i are in their chemical equilibrium, $\Delta G = RT \ln \gamma = 0$ for the chemical reaction $ATP \rightleftharpoons ADP + P_i$, then (eq 16)

$$\langle t_+ \rangle(n) = \langle t_- \rangle(n), \quad \frac{p_+(n)}{p_-(n)} = \frac{n_0 - n}{n} K_{eq} \quad (3)$$

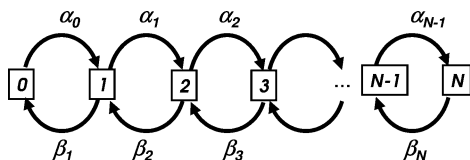


FIGURE 4: A conceptual model for sequential events of phosphorylation and dephosphorylation of a substrate protein R with N copies. The state n represents the number of proteins in the phosphorylated form. That is n R^* and $(N - n)$ R . The difference between this model and that in Figure 2B is that here we do not detail the waiting time distribution. Rather for each state, there is a lumped rate for going forward α_n and a lumped rate for going backward β_n . Note that the states along the chain are “neighbors” in time, not space.

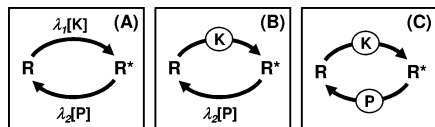


FIGURE 5: Three different types of PdPC with increasing sensitivity in the level of R phosphorylation as a function of the kinase activity (or concentration). (A) Independent system: Both kinase K and phosphatase P are nonsaturating. (B) Semisequential system: The kinase is saturated but not the phosphatase. (C) Strictly sequential system: Both kinase and phosphatase are saturated. In terms of the random walk in Figure 4, one has (A) $\alpha_n = (N - n)\lambda_1[K]$, $\beta_n = n\lambda_2[P]$; (B) $\alpha_n = V_{\max}^K$, $\beta_n = n\lambda_2[P]$; (C) $\alpha_n = V_{\max}^K$, $\beta_n = V_{\max}^P$.

where K_{eq} is the equilibrium constant for the protein phosphorylation reaction: $R + ATP \rightleftharpoons R^* + ADP$, which has to be the same as the equilibrium constant for the dephosphorylation $R + Pi \rightleftharpoons R^*$.

(3) For the cellular environment, the $\Delta G \approx 12$ kcal/mol, $\gamma \approx 4.9 \times 10^8$ (27). We can reasonably assume both kinase and phosphatase are irreversible. Under this condition, $p_+(n)/p_-(n) \propto (n_0 - n)/n$ still, but $\langle t_+(n) \rangle \neq \langle t_-(n) \rangle$ (eqs 23 and 24). If one considers the rate of jumping forward, $\alpha_n = p_+(n)/\langle t_+(n) \rangle$, the probability per unit time, we see that α_n is essentially independent of n . At the same time, since the phosphatase is assumed to be nonsaturating, $\beta_n = p_-(n)/\langle t_-(n) \rangle \propto n$.

RANDOM-WALK REPRESENTATION AND LINEAR COOPERATIVITY

The above analysis suggests the possibility to simplify the two distributions $w_{\pm}(t|n)$ in Figure 2B by two rates α_n and β_n . To better understand the sensitive, cooperative nature of the PdPC activation, we now introduce an even more simplified, conceptual model shown in Figure 4.

We shall show that the conceptual model in Figure 4 is able to clearly demonstrate the essential features of three different types of systems shown in Figure 5: (A) an independent PdPC system; (B) zeroth-order ultrasensitivity with only saturating kinase; and (C) PdPC with both saturating kinase and phosphatase. All three models in Figure 5 can be represented in a sequential kinetic scheme shown in Figure 4. The differences are in the details of the values of α_n and β_n (see below).

To reiterate, understanding the cooperativity in the PdPC requires one to see how the phosphorylation of one substrate protein influences the phosphorylation of another. Therefore, the kinetic scheme in Figure 4 explicitly shows the number of substrate molecules being phosphorylated: from 0 to N ,

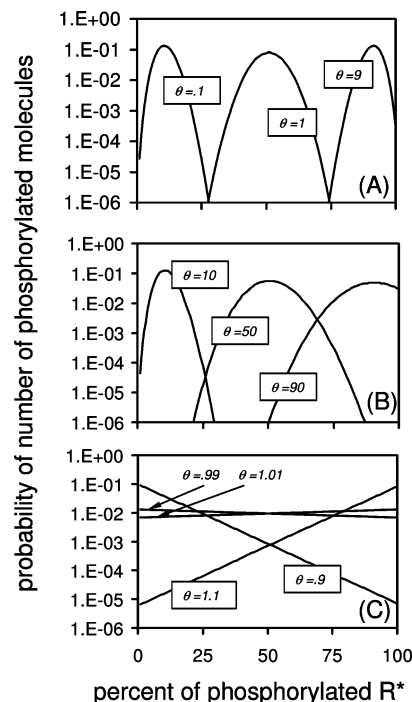


FIGURE 6: Probability distributions of l substrate molecules, among total $N = 100$, in the phosphorylated state. (A) Independent system: $\theta = 0.11, 1$, and 9 , corresponding to the mean of the distribution $\langle l \rangle = 10, 50, 90$. That is mean fraction $f = 0.1, 0.5$, and 0.9 , respectively. From 10% to 90%, the θ changes by a factor of 81. (B) Semisequential system: $\theta = 10, 50, 90$, corresponds to $\langle l \rangle = 10, 50, 90$. From 10% to 90%, the θ changes by a factor of 9. (C) Strictly sequential system: $\theta = 0.9, 0.99, 1.01$, and 1.1 , corresponding to the mean of the distribution $\langle l \rangle = 10, 45, 55$, and 90 . From 10% to 90%, the θ changes by a factor of 1.2. This is ultrasensitivity.

where N is the total number of substrate molecules (i.e., $N/V = R_t$ where V is the volume of the system).

The results presented in the following sections can be simply summarized as follows: For (A) in Figure 5 the probability for the number of R^* being l among total N substrate molecules is binomial distribution with mean $N\lambda_1[K]/(\lambda_1[K] + \lambda_2[P])$. For (B) with large N the distribution is Poisson with mean $V_{\max}^K/\lambda_2[P]$. For (C) the distribution is geometric, $p_l \propto \theta^l$ with $\theta = V_{\max}^K/V_{\max}^P$. Figure 6 shows the probability distributions of the number of phosphorylated R^* .

(A) *Independent System: First-Order PdPC.* Each substrate molecule fluctuates between its R and R^* forms. If there are sufficient numbers of kinase molecules and phosphatase molecules, then the fluctuations of one molecule are independent of other substrate molecules. This is the case if both phosphorylation and dephosphorylation reactions are first order, and the (pseudo first order) rate constants for the reactions are $\lambda_1[S]$ and $\lambda_2[P]$, respectively. Therefore, the α_n and β_n in Figure 4 are directly related to the rate constants $\alpha_n = (N - n)\lambda_1[K]$, $\beta_n = n\lambda_2[P]$. The factor $(N - n)$ in α_n accounts for the phosphorylation of one molecule among $(N - n)$ unphosphorylated R 's; and similarly, the factor n in β_n accounts for the dephosphorylation of one molecule among n phosphorylated R^* 's.

The most important consequence of the completely independent substrate PdPC is that the system can be understood in terms of the reaction of a single substrate protein: $R \rightleftharpoons R^*$. The probability of being R^* is $p^* = \theta/(1$

+ θ) and being R is $1/(1 + \theta) = 1 - p^*$, $\theta = \lambda_1[K]/\lambda_2[P]$. Then for the N substrate molecules, the probability of having l molecules of R^* among them is a binomial distribution:

$$p_l = \frac{N!}{l!(N-l)!} (p^*)^l (1-p^*)^{N-l} \quad (4)$$

The distribution has a single peak around its mean Np^* . The mean fraction of molecules in the R^* is precisely $f = p^*$. When θ increases from 0 to ∞ , p^* increases from 0 to 1, and the peak position of p_l increases accordingly from 0 to N . This is very different from the case of ultrasensitive system in which the distribution has the peak either at 0 or at N , but not in between (see Figure 6C).

Any deviation of the α_n and β_n from this situation is a consequence of certain interactions between the different substrate molecules in their PdPC reactions. For example, in the case of zeroth-order reactions for both kinase and phosphatase, $\alpha_n = V_{\max}^K$ of the kinase and $\beta_n = V_{\max}^P$ of the phosphatase. Hence they are no longer functions of n . To illustrate this, consider there is a single kinase molecule and a single phosphatase molecule, together with N substrate molecules. Then the phosphorylation is strictly sequential, there is a competition for the binding site of the kinase among all the unphosphorylated substrate molecules, and similarly, there is a competition for the binding site of the phosphatase among all the phosphorylated proteins.

(B) Semisequential System: Zeroth-Order Phosphorylation and First-Order Dephosphorylation. The above discussion suggests that if only kinase but not the phosphatase is operating under zeroth-order condition, then one should still observe cooperativity in the PdPC, though to a lesser extent (Figure 5B).

For zeroth-order phosphorylation we have $\alpha_n = V_{\max}^K$ of the kinase, independent of n . We still have $\beta_n = n\lambda_2[P] = n\beta_1$ for the first-order dephosphorylation. Then the probability of having l R^* among N total substrate molecules (eq 27) is $p_l = \theta^l / (l!Z(\theta))$, where $\theta = V_{\max}^K / \beta_1$ represents kinase activity (or concentration).

Again, the distribution has a single peak, around $l = \theta$. Hence, with increasing θ , the peak moves accordingly. The mean fraction of phosphorylated R^* , f , however, no longer coincides with the peak. It increases with θ but gradually lags behind and eventually plateaus. This is exactly what one obtains from the deterministic model, shown in Figure 3A. The random-walk model predicts the same behavior for the mean $f(\theta)$ that is consistent with the deterministic model. The midpoint of the $f(\theta)$ in Figure 3A, $\theta_{1/2}$ at which $f(\theta_{1/2}) = 0.5$, and the Hill's coefficient, n_h , both increase with the N (Figure 7). For large N , the $f(\theta)$ reaches 50% at $\theta_{1/2} = N/2$. The n_h increases with N and plateaus at 2. A similar argument applies to the situation in which kinase is in excess but phosphatase saturated. There one can also reach $n_h = 2$.

(C) Strictly Sequential System: Zeroth-Order PdPC. For both zeroth-order kinase and phosphatase, we have $\alpha_n = V_{\max}^K$ and $\beta_n = V_{\max}^P$, the maximum velocities for the kinase and phosphatase, respectively. Then the probability of having l R^* among total N total substrate molecules (eq 28) is

$$p_l = \frac{(1-\theta)\theta^l}{1-\theta^{N+1}} \quad (5)$$

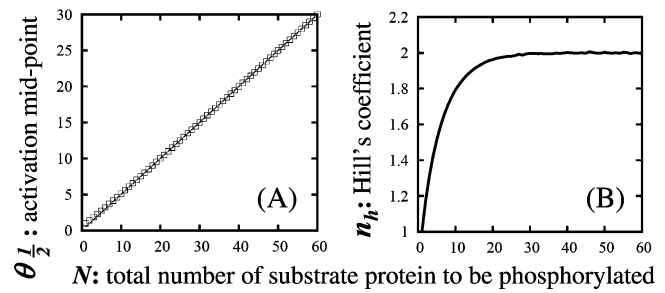


FIGURE 7: Activation curve for semisequential system, $f(\theta)$ given in eq 28, has its Hill's coefficient n_h and midpoint $\theta_{1/2}$ both increase with N : the total number of substrate protein molecules per kinase. Increasing N means increasing saturation of the kinase. The n_h reaches 2 for a highly saturated kinase.

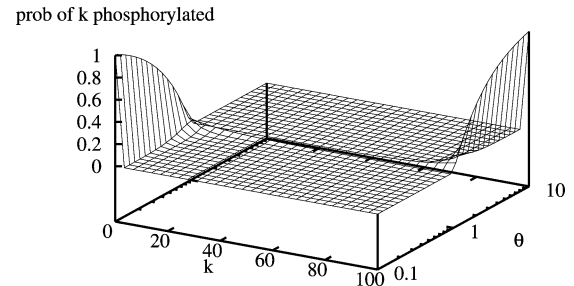


FIGURE 8: In zeroth-order PdPC, an abrupt switching of the peak position for the distribution of the number of phosphorylated molecules, p_k given in eq 5 with $N = 100$. For $\theta < 1$, the peak is located at $k = 0$, but when $\theta > 1$, the peak is located at $k = N = 100$.

This distribution is fundamentally different from those in the previous two cases: The peak of the distribution remains at 0 when θ is increasing from 0 to 1. Then it moves abruptly from 0 to N when $\theta > 1$ and remains. Figure 8 shows the ultrasensitive switching with $N = 100$. Either none of the protein molecules are phosphorylated, when $\theta < 1$, or all of them are phosphorylated, when $\theta > 1$. The Hill's coefficient is $n_h \approx (N + 2)/3$. With large N , the zeroth-order PdPC can be extremely sensitive (4).

APPLICATIONS TO T-CELL ACTIVATION

The concept of temporal cooperativity in terms of the random-walk model is not limited to PdPC and kinetically isomorphic GTPases, but also applies to many other signaling processes. Here we give one example.

Serial Engagement and Triggering Mechanism. The activation of many T-cell receptors (TCR) by binding of antigen-MHC complexes on antigen-presenting cells (APC) has attracted great attention over the years (15). Originally, the researchers were mainly considering the equilibrium binding of the antigen-MHC complex to TCR leading to the activation. Constrained by this thinking, it was puzzling that a low number of MHC complexes could induce the phosphorylation of many TCRs. This led to the proposal of *serial engagement model* which suggested the possibility that a TCR can remain activated after a transient interaction with an MHC complex (28). In other words, an MHC complex can act as a "catalyst" in the activation of the TCR. Even though the nature of the biochemistry can be something different from PdPC/GTPase, the kinetic is the same.

The distinction between the new and the previous thinking precisely parallels the discussion of the two types of

regulation of enzyme activities, namely, the reversible chemical modification by PdPC and allosteric binding (29). Questions concerning these two types of regulation have been posed earlier (30): “Why have organisms found it advantageous to develop separate mechanisms to control the activity of enzymes, namely, by noncovalent (allosteric) changes in structure mediated by appropriate effectors (binding), and by covalent modifications (via PdPC) of the proteins?” “Why are these two mechanisms, ..., usually superimposed on one another even though the changes in conformation resulting in either activation or inhibition are essentially the same?” Recently, Qian and Beard (31) have articulated the essential difference between these two mechanisms: A noncovalent allosteric change in a protein, e.g., TCR, requires the effectors, e.g., MHC complex, in stoichiometric amount: one effector can only control one protein. In order to achieve amplification using a small number of molecules to control a large population of an enzyme, covalent modification with energy utilization is necessary, and PdPC is one of the best examples.

However, the costs of noncovalent allosteric regulation and the covalent modification are different: the former requires a significant amount of biosynthesis of effectors while the latter needs only a small amount of effector. However, the latter requires an energy consumption, in the form of ATP hydrolysis, during the regulatory processes.

It is not necessary to have a chemical bond breaking and forming to modify a protein. Conformational change brought about by an “enzyme” can do that as well. However, it is important to remember that this can only be accomplished in the presence of ATP hydrolysis. In other words, the biochemical reaction system has to be an open system. This is the essential idea behind the “energy relay model” proposed by Hopfield (32), one of the inventors of the theory of kinetic proofreading.

It therefore becomes clear that the random-walk model in Figure 4 applies to the kinetics of serial engagement. Furthermore, the issue of sensitivity in PdPC is also precisely related to the issue of specificity of T-cell activation between its natural ligand and a lower affinity molecule (agonist). Recall that the θ parameter in the PdPC represents the activity ratio of the kinase and the phosphatase, either from their concentrations or from their specific activities. Hence, “ultrasensitivity” in the present context means with a small decrease in the activity of the MHC complex as “the catalyst”, the activation of the TCR can switch from 100% to essentially zero.

To achieve ultraspecificity by the above mechanism, our theory immediately suggests that there needs to be a zeroth-order recycling mechanism in a T-cell that converts the activated TCR back to nonactive form, in analogy to the dephosphorylation reaction in the PdPC. Indeed, it appears that active TCR complexes are highly dynamic, and associated proteins dissociate with short half-lives, allowing inactivation of the system by phosphatases (33). Together with the strong discrimination between higher and lower affinity ligands due to serial engagement, high sensitivity and selectivity is achieved. Whether the deactivation kinetics is indeed zeroth order, however, remains to be tested.

Kinetic Proofreading Mechanism. Kinetic proofreading is another model that explains the high specificity of T-cell activation, but at a single TCR level (34, 35). Even though

the chemistry and molecular mechanism are completely different from those of serial engagement, the essential idea here again is contained in the random-walk model of Figure 4. In this case, the sequential events are the multiple “modifications” of a single TCR, after binding to an MHC complex.

Even though the kinetic scheme of McKeithan (34) looks different from Figure 4, it can be mapped to the random walk in Figure 4 with identical steady state: $\alpha_{k-1}/\beta_k = k_p/(k_p + k_{-1}) = \theta$ where k_p and k_{-1} are the rate constants for modification and dissociation (34). Therefore, this is a strict sequential system with $\theta < 1$. Hence the probability distribution is given by eq 5. In particular, $p_N \propto \theta^N$. Now if an agonist has a slightly greater dissociation rate, $k'_{-1} > k_{-1}$ where we use the prime to indicate the agonist, then $\theta' < \theta$. Therefore, $p'_N/p_N \propto (\theta'/\theta)^N$ can have an extremely small value for large N . The probability of the agonist arriving at the end of the chain is much smaller than that of the natural ligand, even though the probability of the natural ligand arriving at the end is tiny by itself. This is the tradeoff between specificity and sensitivity in the context of kinetic proofreading model (15). The above discussion can be best understood in terms of the Figure 6C, in which the slopes of the straight lines are $\log \theta$. Therefore, the $\log(p'_N/p_N) = N \log(\theta'/\theta)$: For $\theta' < \theta$, the ratio p'_N/p_N can be as small as any number if N is sufficiently large!

Recall that the phosphorylation potential is a necessary condition for the random walk in Figure 4 to exhibit ultrasensitivity. This energy requirement is a key aspect of Hopfield's original theory on kinetic proofreading. Qian has recently provided a thermodynamic limit on the capability of specificity amplification with a given level of phosphorylation potential (35).

DISCUSSION

While a large literature has been devoted to mathematical modeling of increasingly complex, more realistic signal transduction processes, several basic questions concerning PdPC have never been addressed, or even asked. The foremost one is “what is the simplest possible model from a chemical reaction point of view and its prediction?” According to (4), “ultrasensitive” and “subsensitive” responses are defined with respect to a hyperbolic response. Ultrasensitivity of PdPC switches has been widely discussed in the literature, but it has never been made clear why the hyperbolic response is a natural reference.

We see that if one assumes a PdPC with infinite amount of energy from ATP hydrolysis, and both kinase and phosphatase are nonsaturating, then the activation curve of a PdPC is indeed hyperbolic. Note that, except for the mathematical formula, this result has no biochemical connect to the hyperbolic curve in enzyme kinetics. We discover that the simplest, hyperbolic response of a PdPC is indeed related to independence of the substrate proteins, i.e., noncooperative, while sensitivity with $n_h > 1$ is indeed due to a cooperativity between the successive phosphorylation of substrate proteins.

In the present paper, we develop a mathematical analysis of PdPC with a series of models with increasing complexity. Many of the models are sufficiently simple to be studied exactly without approximations. Clearly, these models are

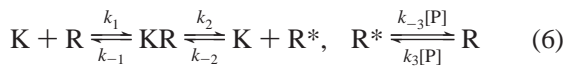
not meant to be realistic for reactions in cells; rather they serve as a part of the language for discussing more realistic PdPC processes, and based on which any more complex models may be built, and to which they may be compared.

As we have demonstrated, the random-walk model is a general theory for signaling sensitivity and specificity. It is not limited to just PdPC and GTPase. Sequential mathematical models as such are a part of the theory of linear cooperativity which had applications in the past ranging from theoretical physics (36) to molecular biophysics to cell biology. For example, the helix formation of DNA and polypeptides (37), protein folding kinetics (38), allosteric cooperativity (29, 39), and actin and microtubule polymerization (40) have all been modeled in terms of linear cooperativity.

The present work has clearly shown that the zeroth-order kinetics for both phosphorylation and dephosphorylation reactions is only one of the necessary conditions for ultrasensitive switch. Having a sufficiently large phosphorylation energy in a living cell is another; and together they are sufficient. Phosphorylation energy is one of the important global quantities for gauging the well-being of cells (27). The realization of this “signal-energy connection” suggests possible new perspectives on signaling pathway aberrations in cellular processes such as apoptosis and tumor growth.

METHODS

Enzyme Kinetics of PdPC. The detailed kinetic equations corresponding to the reaction network in Figure 2A, with sufficient abundance of phosphatase, thus nonsaturating dephosphorylation reaction, is



The sufficient abundance of an enzyme is quantified as the enzyme–substrate complex $[ES] \ll E_t$, the total enzyme. Note however that $[ES]/E_t \leq S_t/E_t$ and $[ES]/E_t = K_M[E][S]/E_t \leq K_M[S]$. Hence sufficiency can come from either $S_t \ll E_t$ or $[S] \leq S_t \ll 1/K_M$. The former means excess of enzyme; the latter means nonsaturating regime of Michaelis–Menten kinetics.

The steady-state concentrations for K, R, KR and R^* in eq 6 satisfy the following four equations:

$$k_1[K][R] - k_{-1}[KR] = k_2[KR] - k_{-2}[K][R^*] = k_3[P][R^*] - k_{-3}[P][R] \quad (7a)$$

$$[K] + [KR] = K_t, \quad [R] + [KR] + [R^*] = R_t \quad (7b)$$

in which K_t is the total concentration of the kinase and R_t is the total concentration of the substrate protein. There are four unknown quantities: $[KR]$, $[K]$, $[R]$ and $[R^*]$. Following the standard Michaelis–Menten assumption that $[KR] \ll [R]$ and $[R^*]$, then we have (5)

$$\theta = \frac{(\mu + 1)f - \mu[K_M + 1 - f + \sigma f]}{\left[1 - f - \frac{1}{\mu\gamma}f\right]} \quad (8)$$

in which $f = [R^*]/R_t$ is the fraction of substrates in the phosphorylated form. The parameters

$$\theta = \frac{k_2 K_t}{k_3 [P] R_t}, \quad \mu = \frac{k_{-3}}{k_3}, \quad K_M = \frac{k_{-1} + k_2}{k_1 R_t}, \quad \gamma = \frac{k_1 k_2 k_3}{k_{-1} k_{-2} k_{-3}}, \quad \sigma = \frac{k_{-2}}{k_1} \quad (9)$$

are the activation signal (θ), equilibrium constant for dephosphorylation (μ), Michaelis constants of the kinase (K_M), and the phosphorylation energy for ATP hydrolysis $\Delta G = RT \ln \gamma$, respectively.

If $\gamma = 1$, then eq 8 is simplified into $f = \mu/(1 + \mu)$, as expected from chemical equilibrium. Under this condition, increasing the concentration of the enzyme kinase, θ , does not affect the equilibrium ratio between the $[R]$ and $[R^*]$ (5, 6).

If both kinase and phosphatase are irreversible, then $k_{-2} = k_{-3} = 0$, then $\mu = \sigma = 0$, $\mu\gamma = \infty$, and $\theta = f(K_M + 1 - f)/(1 - f)$. This yields

$$f = \frac{(K_M + 1 + \theta) - \sqrt{(K_M + 1 + \theta)^2 - 4\theta}}{2} \quad (10)$$

When K_M also is very small, we have $f = \theta$ when $\theta \leq 1$ and $f = 1$ when $\theta \geq 1$.

To characterize the sensitivity of the activation, f , as a function of the signal θ , we borrow the terminology “Hill’s coefficient” from allosteric cooperativity, and define (6, 29)–According to this definition, the n_h for eq 8 is

$$n_h = 2 \left(\frac{d \ln f}{d \ln \theta} \right)_{f=0.5} \quad (11)$$

$$n_h = 2 \left[\frac{2\mu(\gamma - 1)}{(1 - \mu)(\mu\gamma - 1)} - \frac{1 - \sigma}{1 + \sigma + 2K_M} \right]^{-1} \quad (12)$$

The maximal value for the first term in the brackets is 2 (6). If the K_M is very large, the second term is negligible, and then the $n_h = 1$. However, if K_M is very small and $\sigma = 0$, then the second term in the bracket is 1. This corresponds to $n_h = 2$, a factor of 2 in sensitivity amplification due to zeroth-order kinase. It can be shown that $f(\theta)$ in eq 8 has a negative curvature, which means $f'(\theta) \leq f(\theta)/\theta$. Therefore, $n_h = 2$ is the upper bound for this type of activation curve.

Derivation of $w_{\pm}(t|n)$ from MMBH Theory. To obtain the $w_{\pm}(t|n)$ in Figure 2B from the enzyme kinetics given in Figure 2A, we introduce the kinetic scheme in Figure 9B. Note that Figure 9A and eq 6 are essentially the same, with one crucial difference: the k ’s become q ’s. The rate constants k_i are concentration based; and the rate constants q_i are number of molecules based. They differ by a factor of V , the system’s volume. Also, $q_{\pm 3} = k_{\pm 3}[P]/V$.

Figure 9B gives the detailed kinetic scheme of how the system moves with +1 or −1 increments in R^* . Solving this kinetics, one obtains the probability of when the system jumps from state $\{mR, nR^*\}$ to states $\{(m - 1)R, (n + 1)R^*\}$ and $\{(m + 1)R, (n - 1)R^*\}$.

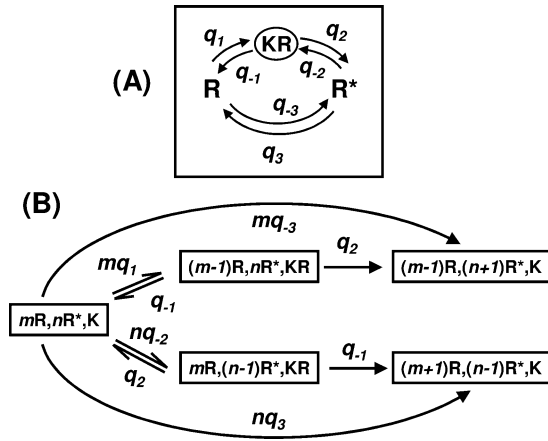


FIGURE 9: (A) The traditional enzyme kinetic scheme for PdPC with kinase catalyzed phosphorylation and nonsaturating phosphatase. (B) Assuming there is only one kinase enzyme molecule, the corresponding stochastic scheme details how the substrate proteins are phosphorylated and dephosphorylated, one at a time.

The master equation for the kinetics in Figure 9B is given by the ODE system

$$\frac{d}{dt} \begin{pmatrix} x_{-2} \\ x_{-1} \\ x_0 \\ x_1 \\ x_2 \end{pmatrix} = \mathbf{A} \begin{pmatrix} x_{-2} \\ x_{-1} \\ x_0 \\ x_1 \\ x_2 \end{pmatrix} \quad (13)$$

in which $x_{-2}, x_{-1}, x_0, x_1, x_2$ represent the probabilities of states $\{(m-1)R, (n+1)R^*, K\}, \{(m-1)R, nR^*, KR\}, \{mR, nR^*, K\}, \{mR, (n-1)R^*, KR\}, \{(m+1)R, (n-1)R^*, K\}$, respectively. The matrix

$$\mathbf{A} = \begin{pmatrix} 0 & q_2 & mq_{-3} & 0 & 0 \\ 0 & -q_2 - q_{-1} & mq_1 & 0 & 0 \\ 0 & q_{-1} & -mq_1 - mq_{-3} - nq_{-2} - nq_3 & q_2 & 0 \\ 0 & 0 & nq_{-2} & -q_{-1} - q_2 & 0 \\ 0 & 0 & nq_3 & q_{-1} & 0 \end{pmatrix} \quad (14)$$

and initial condition is $(0,0,1,0,0)^T$. Equation 13 can be solved by Laplace transform:

$$(s\mathbf{I} - \mathbf{A}) \begin{pmatrix} \tilde{x}_{-2} \\ \tilde{x}_{-1} \\ \tilde{x}_0 \\ \tilde{x}_1 \\ \tilde{x}_2 \end{pmatrix} = \begin{pmatrix} 0 \\ 0 \\ 1 \\ 0 \\ 0 \end{pmatrix} \quad (15)$$

$x_{-2}(t)$ and $x_2(t)$ are the cumulative probability distributions for the forward and backward times, t_+ and t_- . If we let $m = n_0 - n$, then $s\tilde{x}_2(s)$ and $s\tilde{x}_{-2}(s)$ are the Laplace transforms of $w_+(t|n)$ and $w_-(t|n)$ in Figure 2B.

By the Cramer's rule, it can be shown that

$$\frac{\tilde{x}_{-2}(s)}{\tilde{x}_2(s)} = \frac{\begin{vmatrix} q_2 & mq_{-3} & 0 \\ -s - q_2 - q_{-1} & mq_1 & 0 \\ 0 & nq_{-2} & -s - q_{-1} - q_2 \end{vmatrix}}{\begin{vmatrix} -s - q_2 - q_{-1} & mq_1 & 0 \\ 0 & nq_{-2} & -s - q_{-1} - q_2 \\ 0 & nq_3 & q_{-1} \end{vmatrix}} = \frac{m(q_1q_2 + q_2q_{-3} + q_{-3}q_{-1} + sq_{-3})}{n(q_{-1}q_{-2} + q_2q_3 + q_{-1}q_3 + sq_3)} \quad (16)$$

The right-hand-side of eq 16 is independent of s if and only if $q_1q_2q_3/(q_{-1}q_{-2}q_{-3}) = 1$. Then

$$\frac{\tilde{x}_{-2}(s)}{\tilde{x}_2(s)} = \frac{mq_1q_2}{nq_{-1}q_{-2}} = \frac{mq_{-3}}{nq_3} \quad (17)$$

In general, $\gamma = q_1q_2q_3/(q_{-1}q_{-2}q_{-3}) \gg 1$. This corresponds to a large free energy in ATP hydrolysis $\Delta G = RT \ln \gamma$. We have

$$\frac{\tilde{x}_{-2}(0)}{\tilde{x}_2(0)} = \frac{x_{-2}(\infty)}{x_2(\infty)} = \frac{p_+}{p_-} \quad (18)$$

where p_+ and p_- are the probabilities for moving forward and backward, respectively.

To obtain the mean times $\langle t_+ \rangle$ and $\langle t_- \rangle$, we have

$$\langle t_+ \rangle p_+ = \int_0^\infty t dx_{-2}(t) = - \left[\frac{d}{ds} (s\tilde{x}_{-2}(s)) \right]_{s=0} \quad (19)$$

and

$$\langle t_- \rangle p_- = \int_0^\infty t dx_2(t) = - \left[\frac{d}{ds} (s\tilde{x}_2(s)) \right]_{s=0} \quad (20)$$

To simplify the calculation, we now assume that both kinase and the phosphatase are irreversible: $q_{-3} = q_{-2} = 0$. Then the solution to eq 15 is

$$s\tilde{x}_{-2}(s) = \frac{mq_1q_2}{s^2 + (q_2 + q_{-1} + mq_1 + nq_3)s + mq_1q_2 + nq_2q_3 + nq_{-1}q_3} \quad (21a)$$

$$s\tilde{x}_2(s) = \frac{n(q_2 + q_{-1} + s)q_3}{s^2 + (q_2 + q_{-1} + mq_1 + nq_3)s + mq_1q_2 + nq_2q_3 + nq_{-1}q_3} \quad (21b)$$

Therefore,

$$p_+ = \frac{mq_1q_2}{mq_1q_2 + nq_2q_3 + nq_{-1}q_3}, \quad p_- = \frac{n(q_2 + q_{-1})q_3}{mq_1q_2 + nq_2q_3 + nq_{-1}q_3} \quad (22)$$

$$\langle t_+ \rangle = \frac{q_2 + q_{-1} + mq_1 + nq_3}{mq_1q_2 + nq_2q_3 + nq_{-1}q_3}, \quad \langle t_- \rangle = \langle t_+ \rangle - \frac{1}{q_2 + q_{-1}} \quad (23)$$

The forward rate is the ratio of p_+ and $\langle t_+ \rangle$, i.e., the probability per unit time:

$$\alpha = \frac{p_+}{\langle t_+ \rangle} = \frac{mq_1q_2}{q_2 + q_{-1} + mq_1 + nq_3} \quad (24)$$

We see this expression resembles that of Michaelis–Menten. When the kinase is highly saturated, $mq_1 \gg (q_2 + q_{-1})$, then α is independent of m . On the other hand, $\beta = p_-/\langle t_- \rangle$ can be shown to be proportional to n if $q_2 \gg q_{-1}$.

Independent Substrate with First-Order PdPC. For a system with sufficient numbers of kinase molecules and phosphatase molecules, with the substrate proteins undergoing independent PdPC, we have $\alpha_i = (N - i)\lambda_1[K]$ and $\beta_j = j\lambda_2[P]$. If we denote $\theta = \lambda_1[K]/(\lambda_2[P])$, which represents the ratio of activities of kinase to that of phosphatase, then the probability of having l substrates, among total N , being phosphorylated is

$$p_l = \frac{N! \theta^l}{l!(N-l)! Q(\theta)}, \quad Q(\theta) = \sum_{l=0}^N \frac{N! \theta^l}{l!(N-l)!} = (1 + \theta)^N \quad (25)$$

The distribution in eq 25 is in fact a binomial distribution with probability $\theta/(1 + \theta)$ for an individual substrate molecule to be in the R^* state, and $1/(1 + \theta)$ in the R state. The mean number of phosphorylated substrates is $N\theta/(1 + \theta)$, and the fraction of the phosphorylated substrates is $f = \theta/(1 + \theta)$. This hyperbolic curve is the standard for sensitivity in PdPC with respect to which ultrasensitivity is defined. It can be mathematically shown that in eq 10, when $K_M \rightarrow \infty$, we obtain the same hyperbolic response.

Semisequential System. For a semisequential system, which corresponds to a zeroth-order kinase but first-order phosphatase (or vice versa), we have $\alpha_n = V_{\max}^K$ for all n , and $\beta_n = n\beta_1$. The probability distribution is

$$p_l = \frac{\theta^l}{l! Z(\theta)}, \quad Z(\theta) = \sum_{l=0}^N \frac{\theta^l}{l!} \quad (26)$$

in which $\theta = \alpha/\beta_1$. There is no analytical solution for the $Z(\theta)$ in eq 27. Hence, the fraction of phosphorylated substrates has to be evaluated numerically. However,

$$f(\theta) = \frac{1}{N} \frac{d \ln Z(\theta)}{d \ln \theta} = \frac{\theta \sum_{l=0}^{N-1} \theta^l / l!}{N \sum_{l=0}^N \theta^l / l!} \quad (27)$$

For large N , p_l in eq 26 is approximately Poisson with mean θ . Hence mean fraction $f = \theta/N$ when $\theta \leq N$ and 1 when $\theta \geq N$. Furthermore, when $\theta = N/2$, $f = (1/2)$ and $n_h = 2(d \ln f(\theta)/d \ln \theta)_{\theta=N/2} \approx 2 - (\sqrt{e/2})^N$. This agrees with that in Figure 7B.

Strictly Sequential System with Zeroth-Order PdPC. For a strictly sequential system we have both $\alpha_n = V_{\max}^K$ and $\beta_n = V_{\max}^P$ independent of n . Again, let $\theta = V_{\max}^K/V_{\max}^P$. The probability p_l then is

$$p_l = \frac{\theta^l}{\Xi(\theta)}, \quad \Xi(\theta) = \sum_{l=0}^N \theta^l = \frac{1 - \theta^{N+1}}{1 - \theta} \quad (28)$$

The fraction of phosphorylated substrates, then, is

$$f(\theta) = \frac{1}{N} \frac{d \ln \Xi(\theta)}{d \ln \theta} = \frac{\theta(1 - (N+1)\theta^N + N\theta^{N+1})}{N(1 - \theta)(1 - \theta^{N+1})} \quad (29)$$

and

$$\frac{df}{d\theta} = \frac{(1 - \theta^{N+1})^2 - (N+1)^2(1 - \theta)^2\theta^N}{(1 - \theta)^2(1 - \theta^{N+1})^2} \quad (30)$$

For sufficiently large $N \gg 1$,

$$f(\theta) = \frac{1}{2} + \frac{N+2}{12}(\theta - 1) + O((1 - \theta)^2) \quad (31)$$

indicating that $f = 1/2$ when $\theta = 1$. Therefore, the Hill's coefficient $n_h = 2(d \ln f(\theta)/(d \ln \theta))_{\theta=1} = (N+2)/3$.

ACKNOWLEDGMENT

We are grateful to one of the anonymous reviewers for suggesting to include Figure 8. We thank Daniel Beard, Hao Ge, Byron Goldstein, James Hurley, Martin Kushmerick, Guangpu Li, Jin Wang, and Jianhua Xing for helpful discussions.

REFERENCES

1. Krebs, E. G., and Beavo, J. A. (1979) Phosphorylation-dephosphorylation of Enzymes, *Annu. Rev. Biochem.* 48, 923–959.
2. Cooper, J. A., and Howell, B. (1993) The when and how of src regulation, *Cell* 73, 1051–1054.
3. Stadtman, E. R., and Chock, P. B. (1977) Superiority of interconvertible enzyme cascades in metabolic regulation: Analysis of monocyclic systems, *Proc. Natl. Acad. Sci. U.S.A.* 74, 2761–2765.
4. Goldbeter, A., and Koshland, D. E. (1981) An amplified sensitivity arising from covalent modification in biological systems, *Proc. Natl. Acad. Sci. U.S.A.* 78, 6840–6844.
5. Qian, H. (2003) Thermodynamic and kinetic analysis of sensitivity amplification in biological signal transduction, *Biophys. Chem.* 105, 585–593.
6. Qian, H. (2007) Phosphorylation energy hypothesis: open chemical systems and their biological functions, *Annu. Rev. Phys. Chem.* 58, 113–142.
7. Gonze, D., and Goldbeter, A. (2001) A model for a network of phosphorylation-dephosphorylation cycles displaying the dynamics of dominoes and clocks, *J. Theor. Biol.* 210, 167–186.
8. Heinrich, R., Neel, B. G., and Rapoport, T. A. (2002) Mathematical models of protein kinase signal transduction, *Mol. Cell* 9, 957–970.
9. LaPorte, D. C., and Koshland, D. E. (1983) Phosphorylation of isocitrate dehydrogenase as a demonstration of enhanced sensitivity in covalent regulation, *Nature* 305, 286–290.
10. Shacter, E., Chock, P. B., and Stadtman, E. R. (1984) Regulation through phosphorylation/dephosphorylation cascade, *J. Biol. Chem.* 259, 12252–12259.
11. Meinke, M. H., Bishop, J. S., and Edstrom, R. D. (1986) Zero-order ultrasensitivity in the regulation of glycogen phosphorylase, *Proc. Natl. Acad. Sci. U.S.A.* 83, 2865–2868.
12. Kim, S. Y., and Ferrell, J. E. (2007) Substrate competition as a source of ultrasensitivity in the inactivation of Wee1, *Cell* 128, 1133–1145.
13. Bourne, H. R., Sanders, D. A., and McCormick, F. (1990) The GTPase superfamily: a conserved switch for diverse cell functions, *Nature* 348, 125–131.
14. Li, G. P., and Qian, H. (2003) Sensitivity and specificity amplification in signal transduction, *Cell Biochem. Biophys.* 39, 45–60.

15. Goldstein, B., Faeder, J. R., and Hlavacek, W. S. (2004) Mathematical and computational models of immune-receptor signaling, *Nat. Rev. Immunol.* **4**, 445–456.
16. Tan, Y.-C., Wang, W.-N., Zheng, Y., and Wang, Z.-X. (2008) Zero-order ultrasensitivity in the GTP-binding and GTP-hydrolysis cycle of Rac1 GTPase, manuscript in preparation.
17. Demotz, S., Grey, H. M., and Sette, A. (1990) The minimal number of class II MHC-antigen complexes needed for T cell activation, *Science* **249**, 1028–1030.
18. Qian, H., and Xie, X. S. (2006) Generalized Haldane equation and fluctuation theorem in the steady state cycle kinetics of single enzymes, *Phys. Rev. E* **74**, 010902(R).
19. Zhu, G., Zhai, P., Liu, J., Terzyan, S., Li, G., and Zhang, X. C. (2004) Structural basis of Rab5-Rabaptin5 interaction in endocytosis, *Nat. Struct. Mol. Biol.* **11**, 975–983.
20. Kennedy, M. J., Dunn, F. A., and Hurley, J. B. (2004) Visual pigment phosphorylation but not transducin translocation can contribute to light adaptation in zebrafish cones, *Neuron* **41**, 915–928.
21. Qian, H. (2006) Open-system nonequilibrium steady-state: statistical thermodynamics, fluctuations and chemical oscillations, *J. Phys. Chem. B* **110**, 15063–15074.
22. Beard, D. A., and Qian, H. (2008) *Chemical Biophysics: Quantitative Analysis of Cellular Systems*, Cambridge Univ. Press, New York.
23. Wang, H., and Qian, H. (2007) On detailed balance and reversibility of semi-Markov processes and single-molecule enzyme kinetics, *J. Math. Phys.* **48**, 013303.
24. Kolomeiskey, A. B., and Fisher, M. E. (2000) Extended kinetic models with waiting-time distributions: exact results, *J. Chem. Phys.* **113**, 10867–10877.
25. Flomenbom, O., and Klafter, J. (2005) Closed-form solutions for continuous time random walks on finite chains, *Phys. Rev. Lett.* **95**, 098105.
26. Qian, H., and Wang, H. (2005) Continuous time random walks in closed and open single-molecule systems with microscopic reversibility, *Europhys. Lett.* **76**, 15–21.
27. Kushmerick, M. J. (1998) Energy balance in muscle activity: simulations of ATPase coupled to oxidative phosphorylation and to creatine kinase, *Comp. Biochem. Physiol. B* **120**, 109–123.
28. Valitutti, S., Muller, S., Cella, M., Padovan, E., and Lanzavecchia, A. Serial triggering of many T-cell receptors by a few peptide-MHC complexes, *Nature* **375**, 148–151 (1995).
29. Wyman, J., and Gill, S. J. (1990) *Binding and Linkage: Functional Chemistry of Biological Macromolecules*, Univ. Sci. Book, Mill Valley, CA.
30. Fischer, E. H., Heilmeyer, L. M. G., and Haschke, R. H. (1971) Phosphorylase and the control of glycogen degradation, *Curr. Top. Cell. Regul.* **4**, 211–251.
31. Qian, H., and Beard, D. A. (2006) Metabolic futile cycles and their functions: a systems analysis of energy and control, *IEE Proc. Syst. Biol.* **153**, 192–200.
32. Hopfield, J. J. (1980) The energy relay: a proofreading scheme based on dynamic cooperativity and lacking all characteristic symptoms of kinetic proofreading in DNA replication and protein synthesis, *Proc. Natl. Acad. Sci. U.S.A.* **77**, 5248–5252.
33. Bunnell, S. C., Hong, D. I., Kardon, J. R., Yamazaki, T., McGlade, C. J., Barr, V. A., and Samelson, L. E. (2002) T cell receptor ligation induces the formation of dynamically regulated signaling assemblies, *J. Cell Biol.* **158**, 1263–1275.
34. McKeithan, T. W. (1995) Kinetic proofreading in T-cell receptor signal-transduction, *Proc. Natl. Acad. Sci. U.S.A.* **92**, 5042–5048.
35. Qian, H. (2006) Reducing intrinsic biochemical noise in cells and its thermodynamic limit, *J. Mol. Biol.* **362**, 387–392.
36. Lieb, E. H., and Mattis, D. C. (1966) *Mathematical Physics in One Dimension: Exactly Soluble Models of Interacting Particles*, Academic Press, New York.
37. Qian, H., and Schellman, J. A. (1992) Helix-coil theories: a comparative studies for finite length polypeptides, *J. Phys. Chem.* **96**, 3987–3994.
38. Elson, E. L. (1972) Simple sequential model for the kinetics of conformational transitions of oligomeric helices and proteins, *Biopolymers* **11**, 1499–1520.
39. Hill, T. L. (1985) *Cooperativity Theory in Biochemistry*, Springer-Verlag, New York.
40. Hill, T. L. (1987) *Linear Aggregation Theory in Cell Biology*, Springer-Verlag, New York.

BI702125S